# Testing optical telescopes from defocused stellar images

C. Roddier,
J.E. Graves, M.J. Northcott, F. Roddier

Institute for Astronomy, University of Hawaii
2680 Woodlawn Drive, Honolulu, Hawaii 96822

## ABSTRACT

Wave-front reconstruction from defocused stellar images has now been widely applied to the testing of ground-based optical telescopes. We describe here the latest improvements to the technique and discuss how to reach a maximum accuracy. Statistics are given on the aberrations observed over 10 different telescopes.

## 1. INTRODUCTION

Several techniques can be applied to the reconstruction of wave fronts from images taken at various focus positions. Phase retrieval algorithms are widely applied to millimetric telescopes [1] and have been successfully applied to the determination of the aberrations of the Hubble Space Telescope [2, 3]. However, the technique is limited to monochromatic point sources and cannot be applied to long exposure stellar image blurred by seeing. More general phase diversity methods have been proposed [4, 5, 6] but none of them has yet been used in practice. Recently [7] we developed an algorithm which works on images sufficiently defocused to be outside the caustic zone. It requires at least two images defocused in opposite directions. The technique can be used to reconstruct wave-fronts from long exposure stellar images taken through the atmosphere. It has now been extensively applied to the testing of optical telescopes at various observatories. We present here recent attempts to further improve its accuracy and spatial resolution, and review results obtained over 7 telescopes 3-m or larger in diameter and 3 telescopes in the 2 to 3-m range.

## 2. DATA ACQUISITION

Most telescopes are now equipped with science-grade CCD cameras which can be used for that purpose. With an all reflecting telescope, no color filter is needed. Experience shows that an exposure time of at least 30 seconds to one minute is necessary to average out seeing effects. To avoid saturating the CCD, a sufficiently defocused 8-mag star from the Smithsonian Astrophysical Observatory (SAO) catalog is generally appropriate.

A critical parameter is the distance to focus at which images are taken. This distance is chosen by trading sensitivity against spatial resolution. The larger is the amount of defocus the higher is the spatial resolution on the reconstructed wave front, but the lower is the sensitivity to aberrations. A defocused stellar image can be viewed as a blurred pupil image. To a good approximation the amount of blur is given by the size of the in-focus image. The ratio of the diameter of the defocused image over the diameter of the best focused image is therefore a measure of the maximum number of resolved wave-front elements across a pupil diameter. A value of at least 40 resolution elements is generally considered as acceptable. Our experience is that good results are usually obtained when the spider arms are clearly visible on both images whereas the effect of the aberrations are barely visible. For best results, it is advisable to take several images with various amounts of defocus. The algorithm should give the same result on all the images over a wide range of distances.

 0-8194-1494-8/94/$6.00

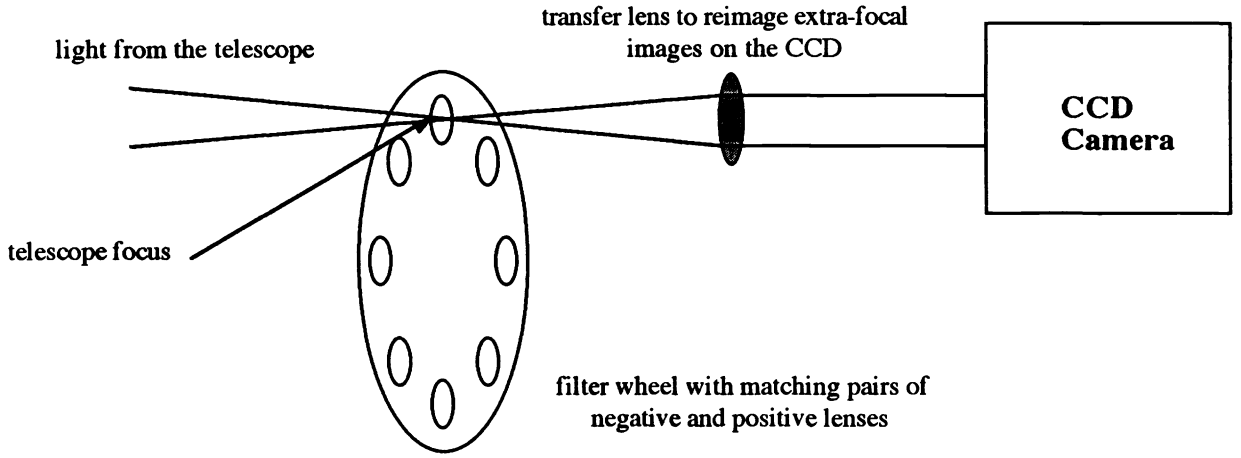


**Fig. 1.** Optical set-up to record extrafocal images on a CCD camera.

## 3. USE OF LENSES

A problem occurs when the testing has to be made on a slow beam such as provided by most infrared telescopes or infrared foci of optical telescopes. For instance the 3-m Infrared Telescope Facility (IRTF) on Mauna Kea has an f/35 Cassegrain focus with a plate scale of almost 2 arc-second/millimeter. Assuming one arc-second in-focus images, getting 40 resolution elements per pupil diameter requires a CCD chip at least 20 mm wide, which is seldom available especially on infra-red telescopes. With just a few simple lenses one can focus onto a CCD extra-focal images at any distances without moving the camera or telescope secondary (Fig. 1). A great advantage is also realized because the image on the CCD does not change size with extra-focal distance. In practice a set of matching lens pairs are mounted in a filter wheel, that cover the desired range. Unless severe aberrations are present, focal lengths are chosen in a range of 250 mm to 2000 mm. The second element serves to image the telescope pupil on the CCD when no lens exist in the image plane. Its focal length determines the size of the images. When either a positive or negative lens is inserted in the focal plane, the pupil image is defocused and an extrafocal image is formed on the CCD. The extrafocal distance is equal to the focal length of the inserted lens. A positive lens produces an inside focus image, a negative lens an outside focus image. Such a device has been built at the United Kingdom Infrared Telescope (UKIRT) and has since been widely used to map the aberrations of the telescope as a function of its orientation.

## 4. PRIME FOCUS VERSUS CASSEGRAIN FOCUS

For a number of telescopes, we have data taken both at the prime focus and at the Cassegrain focus. In the case of Ritchey Chrétien telescopes, prime focus data were taken without corrector but with a large amount of defocus to minimize the effect of spherical aberration. Fig. 2 shows a comparison between wave fronts reconstructed from prime focus data (left) and from Cassegrain focus data (right). The first 23 Zernike terms have been removed to show only the small scale wave-front deformations. The similarity of the two images show that small scale wave-front deformations are almost entirely produced by the telescope primary mirror. This is almost always the case. This is because wave-front deformations produced by the secondary are scaled up as the ratio of the mirror diameter; hence, it is easier to manufacture a good small mirror than a large one. Only for one telescope did we found a significant contribution of the secondary.

In Fig. 2, the right side image appears blurred compared to the left side image. This is because data were taken comparatively closer to focus. To get comparable results, the distance to focus must be taken proportional to the square of the f-ratio, and this was not the case. Fig. 3 shows the same cross-section for the two reconstructed wave front. Both show the same wave-front deformation, but because of the lower resolution of the Cassegrain data, the associated rms wave-front deformation appears to be smaller. This emphasizes the importance of spatial resolution in the estimation of the rms wave-front deformation. Generally Shack-Hartmann data do not have the resolution of the data presented here, and the rms wave front deformation is even more underestimated. Small scale wave-front deformations scatter lights and put a limit on the detectability of faint objects close to a bright star.

**Fig. 2.** Gray level display of the wave-front phase reconstructed from prime focus data (left) and from Cassegrain focus data (right). 23 low order Zernike terms have been removed to show only the small scale wave-front deformation. The similarity of the two images show that small scale wave-front errors are almost entirely produced by the telescope primary mirror.

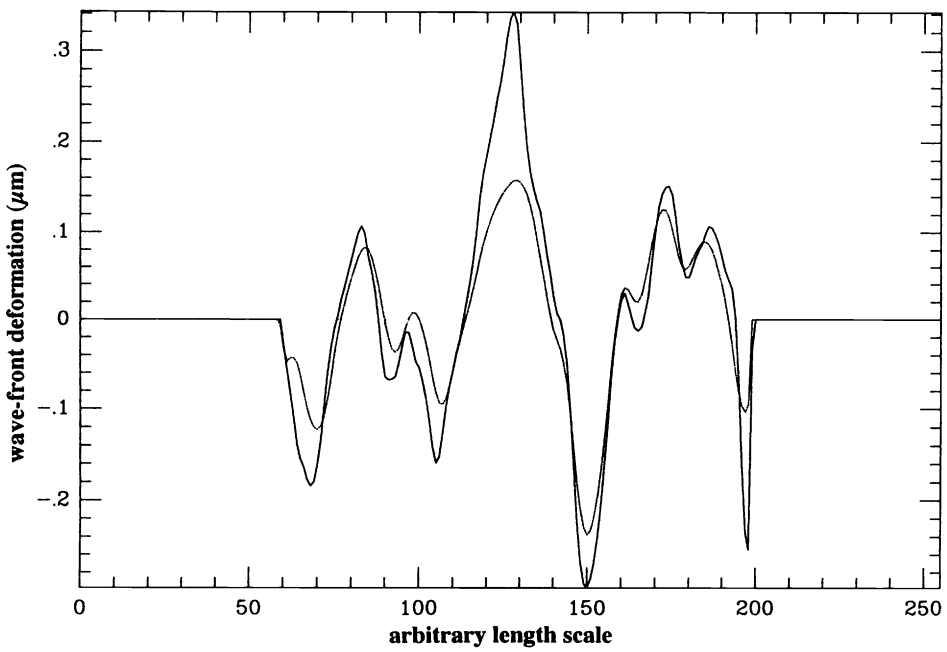


**Fig. 3.** Cross section of the wave-front surfaces shown in Fig. 2. Full line: prime focus data. Dotted line: Cassegrain focus data. In the latter, the wave-front rms distortion is underestimated owing to a lower resolution.

Results on lower order aberration terms are more difficult to compare because these terms often depend on the orientation of the telescope and on the accuracy of the optical alignment, and therefore vary with time. However, spherical aberration is a quite stable term and in several occasions we have been able to determine the contribution of the secondary to spherical aberration. Most telescopes show negative spherical aberration apparently due to a systematic error in the conical constant of the primary. On Mauna Kea, the Canada-France-Hawaii telescope (CFHT), which has a parabolic mirror, has less spherical aberration at the Cassegrain focus than at the prime focus, because a back pressure is applied to the secondary and fine tuned to adjust the conical constant. In two occasions our measurements have been used, either alone (UH 88") or in addition to Shack-Hartmann tests (CTIO 4-m), to specify the conical constant of a new secondary. It practically eliminated the spherical aberration term at the Cassegrain focus.

## 5. FITTING ZERNIKE POLYNOMIALS

Reconstructed wave-fronts are often described in terms of aberrations coefficients. These are generally the coefficients of a Zernike expansion. However, care is not always taken to chose Zernike functions which are precisely orthogonal over the considered pupil area. The expansion is often done with regular Zernike functions which are orthogonal only over a full circular pupil. This can be quite detrimental to the accuracy of the results. We found significant differences when the central obstruction ratio is equal or larger than 0.3. Moreover, because of the lack of orthogonality, results depend on the number of estimated terms.

This is particularly important when one wants to estimate a conical constant. In this case, one wants to measure the spherical aberration coefficient with a good accuracy. A problem arises because most mirrors have a turned edge. Hence, one may wish to measure the spherical aberration over the best part of the mirror only. We found that small changes on the area over which the fit is made produce large variations on the value of the regular Zernike coefficient, up to a factor two. However, when the expansion is done over Zernike functions which are orthogonal over the area on which the fit is made, the variations are much smaller.

It must be emphasized that the same problem occurs with the Hartmann test as discussed by Bhatia et al. (1993) as well as others. As wave-front reconstruction methods are becoming increasingly accurate, it becomes increasingly necessary to expand the reconstructed wave front over a basis of perfectly orthogonal functions.

## 6. GENERAL RESULTS

As already indicated above, the low order aberration terms have a different behavior from the high order terms. We found the high order terms extremely stable. For instance using data taken at the IRTF prime focus, we have removed the low order Zernike terms and mapped the residual wave-front slopes. Features seen on the maps are strikingly similar to that seen on photographs taken in Foucault (or knife-edge) tests made at the optical shop for the primary mirror acceptance tests. Hence, we are confident we can accurately reconstruct the small scale mirror deformations left by the polishing tool. The sensitivity is at least equal and probably greater than that of the Foucault test although the measurements were made in situ through a considerable amount of atmospheric turbulence.

On the contrary, low order terms can vary significantly from one set of measurement to an other. These are true variations which can be easily related to actions taken on the telescope. For instance on most telescopes astigmatism was found to vary with the telescope orientation (right ascension and declination). We found it was in general related to problems in the primary mirror lateral supports. Coma is more independent of the telescope position, but is highly dependent on telescope alignment. Telescopes which have recently installed remote controls for the alignment (CFHT, UH 88") are now found to have less coma and better show their superb optical quality. Most primary mirrors have three fixed point in their supports, and triangular coma tends to appear and disappear depending upon the pressure applied to the primary mirror back supports. Although less variable than astigmatism, the "ashtray" term was also found to be related to forces exerted by the primary mirror lateral supports.

A good measure of the optical quality of an image forming system is given by its Strehl ratio, that is the ratio of the maximum intensity in a point source image to the maximum intensity in a diffraction-limited image. Since we have tested infrared telescopes as well as optical ones, we have chosen to calculate their Strehl ratios at an intermediate wavelength of 0.85 $\mu$m. Fig. 4 shows the Strehl ratios obtained for each of our data set (data taken on the same telescope but at a different

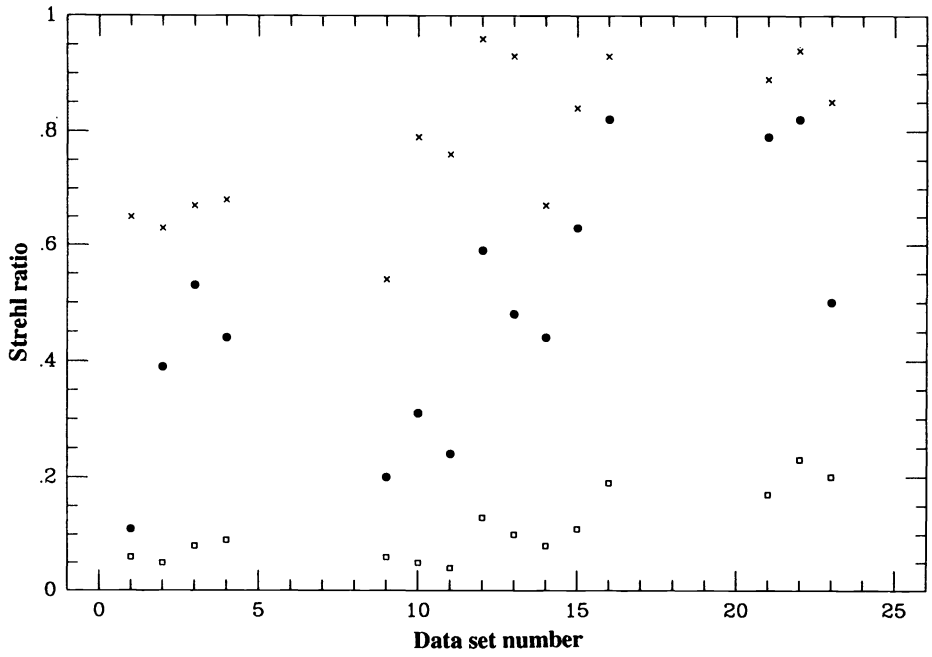


Fig. 4. Strehl ratios computed at 0.85 $\mu$m for each data set. Left group: infrared telescopes. Central group: classical optical telescopes. Right group: actively controlled telescopes. Squares: with all measured aberrations. Full circle: after removal of astigmatism, coma, triangular coma and spherical aberration. Crosses: after removal of 23 low order Zernike terms.

focus are considered as belonging to a different data set). Data set have been grouped in three classes. On the left are the infrared telescopes, in the middle are the classical optical telescopes, on the right are actively controlled telescopes. The squares indicate the Strehl ratio obtained for telescopes as they were. When data were recorded under different alignment positions, we took the best results. We note a superiority (but not overwhelming) of actively controlled telescopes. Full circles show Strehl ratios calculated after removal of astigmatism, coma, triangular coma, and spherical aberration. These are terms over which actions can be taken such as adjusting forces exerted by the primary mirror support (astigmatism, triangular coma) or refining the alignment (coma) and finding the best focus (spherical). Fig. 4 demonstrates the extreme sensitivity of the Strehl ratio to these terms and shows how greatly a telescope can be improved by taking appropriate actions. Finally crosses give Strehl ratios calculated after removal of 23 low order Zernike terms, and essentially indicate the polishing quality of the primary mirror. Infrared telescopes have been clearly polished to a lesser quality than optical telescopes, but not by a large amount.

**Table 1.** Statistics of the aberrations measured over 15 different sets of data taken on 10 different telescopes (rms wave-front distortion in nanometers).

| aberration | average | maximum | minimum |
|---|---|---|---|
| astigmatism | 213 | 550 | 70 |
| coma | 186 | 580 | 50 |
| triangular | 84 | 200 | 30 |
| quadratic | 48 | 140 | 10 |
| spherical (Z11) | 73 | 250 | 1 |
| spherical (Z11+Z22) | 64 | 210 | 10 |
| wavefront (total) | 408 | 800 | 190 |
| residual (-23 Zernikes) | 73 | 150 | 20 |

Table 1 shows for a few low order terms the associated rms wave-front error expressed in nanometers. The last two lines give the total rms wave-front distortion without and with removal of 23 low order Zernike terms. The first column gives the average value for all our data set, the second column the worse value, and the third column the best value. It confirms that the low order terms have a dominant contribution and that a telescope can be greatly improved by proper control of the primary mirror supports and alignment. These are also terms which can be easily controlled by active and adaptive optics.

## 7. CONCLUSION

The technique of wave-front reconstruction from defocused stellar images has been found to be an invaluable diagnostic tool to assess and characterize the optical quality of ground-based telescopes. Compared to the classical Hartmann or Shack-Hartmann tests, it is easier to implement and does not require calibration with a flat reference wave front. It allows us to reconstruct wave fronts with a higher spatial resolution and therefore a greater accuracy. In many cases it has been successfully used to improve the optical quality of astronomical telescopes.

## 8. REFERENCES


1. D. Morris, "Phase retrieval in the radio holography of reflector antennas and radio telescopes," IEE Trans. Antennas Propag. **AP-33**, 749-755 (1985).

2. J.R. Fienup, J.C. Marron, T.J. Schultz, and J.H. Seldin, "Hubble Space Telescope characterized by using phase-retrieval algorithms," Applied Optics 32, 1747-1767 (1993).
3. C. Roddier, F. Roddier, "Combined approach to the Hubble Space Telescope wave-front distortion analysis," Applied Optics **32**, 2992-3008 (1993).

4. R.A. Gonsalves, "Phase retrieval by differential intensity measurements," J. Opt. Soc. Am. A 4, 166-170 (1987).

5. R.G. Paxman and J.R. Fienup, "Optical misalignment sensing and image reconstruction using phase diversity," J. Opt. Soc. Am. A 5, 914-923 (1988).

6. J.R.P. Angel, P. Wizinovich, M. lloyd-Hart, D. Sandler, "Adaptive optics for array telescopes using neural-network techniques," Nature **348**, 221-224 (1990).

7. C. Roddier, F. Roddier, "Wave-front reconstruction from defocused images and the testing of ground-based optical telescopes," J. Opt. Soc. Am. A 10, 2278-2287 (1993).

8. R. Bhatia, A. Ciani, P. Rafanelli, "Results from Shack-Hartmann analysis of the 3.5-m primary mirror of the Galileo telescope," Telescopio Nazionale Galileo Tech. rep. No. 24, Osservatorio Astronomico di Padova, 1993.